

Mutual Coupling Reduction of a (2×1) MIMO Antenna System Using Parasitic Element Structure for WLAN Applications

¹Abdul Ghafor A. Abdul Hameed, ²Abdul Kareem S. Abdullah,

³Haider M. Al Sabbagh, ⁴Hussain K. Bashir

^{1,2,3,4}Department of Electrical Engineering, College of Engineering, University of Basrah, Basra, Iraq

²drasabdallah@ieee.org, ³haidermaw@ieee.org

ABSTRACT

In this paper, a novel parasitic element structure is proposed to reduce the mutual coupling produced in a compact (2×1) multi-input multi-output (MIMO) antenna system working at 2.4 GHz for wireless local area network (WLAN) applications. The proposed structure has a rectangular shape with (10) square slots built using FR-4 substrate with relative permittivity of 4.4 and loss tangent 0.025. The resulted MIMO antenna is found to have a low mutual coupling of about -25dB and an envelope correlation coefficient less than 0.1 in the band of interest. The antenna also has a wide relative bandwidth of 18.75%, high total efficiency of 89.5% and acceptable realized gain of about 2.25dBi.

Keywords: MIMO, parasitic element, ISM band, mutual coupling.

1. INTRODUCTION

In the last years, wireless communications grew very fast specially for WLAN communications, due to the different techniques which have been used to increase the channel capacity by increasing the data rate transform and reduce probability of error [1]. One of the important techniques used for this purpose is the multiple-input multiple-output (MIMO) antenna systems, which utilize the advantages of multiplexing gain and diversity gain [2]. However, these systems have some disadvantages, especially the high mutual coupling that presents between the MIMO elements. The mutual coupling can be attributed to two reasons; the electromagnetic interaction of the elements or the surface current flowing from one element to the other or both [1]. Mutual coupling affects the MIMO antennas characteristics by degrading the impedance matching, reducing the efficiency, decreasing the capacity of the channel, increasing the correlation, increasing the coupling power and reducing the radiated power [3-4].

There are several methods to reduce the mutual coupling; some of them are used to produce single-band or multi-band characteristics. Two orthogonal patches antenna with lower mutual coupling has been designed in [5] for the 2.4 GHz industrial, science and medical (ISM) band. Neutralization line method has been used in [6] to reduce the mutual coupling for the 2.4GHz wireless applications. Split ring resonator (SRR) met material has been used in [7] to produce port to port isolation lower than 15dB. The spacing between the MIMO elements constitutes a challenge, and many researchers tried to find techniques that offer compact sizes along with very high isolation. In [8], parasitic elements were used with spacing of 0.082λ , which produces mutual coupling less than -16dB.

In this paper, the design and analysis of two elements MIMO antenna for ISM band application is presented. A novel parasitic element technique with spacing of 0.048λ between elements is used and very low correlation and higher isolation values between elements were achieved. In Section-2, a single rectangular patch

antenna is designed to operate at 2.4GHz. A slot is introduced in the patch to increase its effective length and decreased its area. In Section-3, MIMO antenna design is presented to decrease the mutual coupling by proposing a novel rectangular shape parasitic element. Conclusion and discussion of the obtained results are presented in Section 4.

2. DESIGN OF SINGLE RECTANGULAR PATCH ANTENNA

A single rectangular patch is firstly designed to resonate at 2.4GHz with inset fed as shown in Figure 1. The dielectric substrate is chosen to be FR4 substrate with dielectric constant $\epsilon_r=4.4$, thickness $h=1.6\text{mm}$, and loss tangent $\tan\delta=0.025$. The dimensions of the patch ($L_{\text{patch}} \times W_{\text{patch}}$) are found as $(38 \times 28.32) \text{mm}^2$ using the following design formulas[9]:

$$W_{\text{patch}} = \frac{1}{2f_r \sqrt{\epsilon_0 \mu_0} \sqrt{\epsilon_r + 1}} \sqrt{\frac{2}{\epsilon_r + 1}} \quad (1)$$

$$L_{\text{patch}} = \frac{1}{2f_r \sqrt{\epsilon_{\text{reff}}} \sqrt{\epsilon_0 \mu_0}} - 2\Delta L \quad (2)$$

where,

f_r : The resonant frequency

ϵ_0 : Free-space permittivity

μ_0 : Free-space permeability

ϵ_{reff} : Effective dielectric constant given by:

$$\epsilon_{\text{reff}} = \frac{\epsilon_r + 1}{2} + \frac{\epsilon_r - 1}{2} \left(1 + 12 \frac{h}{W}\right)^{-1} \quad (3)$$

The line extension ΔL due to fringing field can be given by:

$$\Delta L = 0.412h \frac{(\epsilon_{reff} + 0.3) \left(\frac{W}{h} + 0.264 \right)}{(\epsilon_{reff} - 0.258) \left(\frac{W}{h} + 0.8 \right)} \quad (4)$$

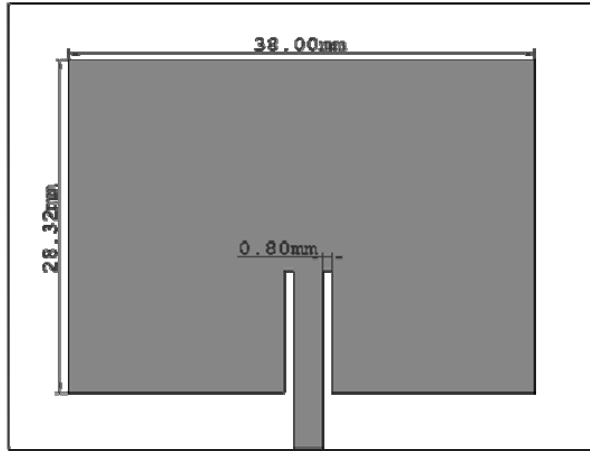


Figure 1: The single rectangular patch antenna

The simulated return loss (in dB) against frequency is plotted in Figure 2. It is clear that the patch has good impedance matching at 2.4GHz with return loss value of -28.5dB. However, its bandwidth is relatively low (about 50MHz), thus it needs to be improved. The partial ground technique [10] is chosen here to improve the bandwidth. By this technique, the capacitance between ground plane and the patch is decreased and the bandwidth is increased consequently.

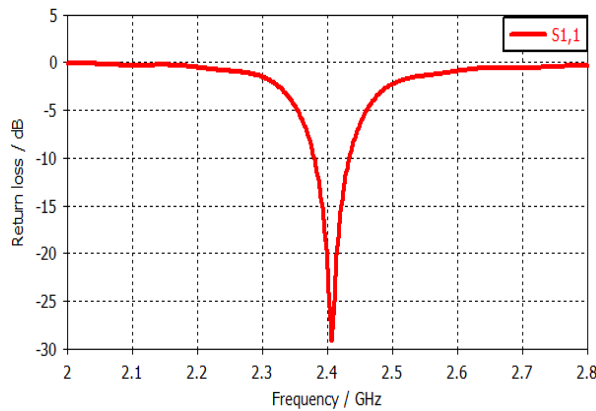


Figure 2: Return loss plot of the single rectangular patch antenna

The dimensions of the radiating patch are relatively big to be used in MIMO system, where the size is very critical parameter. Therefore, a slot is introduced to the radiated patch in order to increase its effective length [11] as shown in Figure 3. The dimensions of this slot has been optimized using CST software package [12] and listed as shown in Table 1.

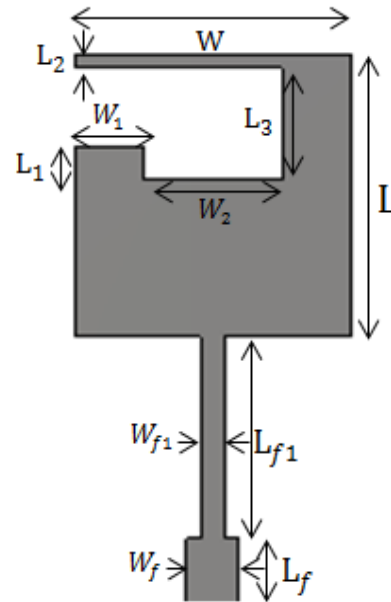


Figure 3: The optimized slotted patch

Table 1: The dimensions of the optimized slotted patch

Parameter	Value(mm)	Parameter	Value(mm)
L	17.3	W	16
L ₁	4.8	W ₁	4
L ₂	0.5	W ₂	8
L ₃	9		

The resonance is maintained at 2.4GHz by using quarter-wavelength matching transform instead of original inset feed with dimensions listed in Table 2.

Table 2: Dimensions of the quarter-wavelength matching transformer

Parameter	Value (mm)
L _f	6
L _{f1}	14.5
W _{f1}	3
W _f	1.4

It is noticeable from Figure 4 that the optimized patch has a minimum reflection coefficient value of about -29dB at 2.4GHz with a large bandwidth of about 485MHz (i.e. percentage increase of 20.2%).

http://www.cisjournal.org

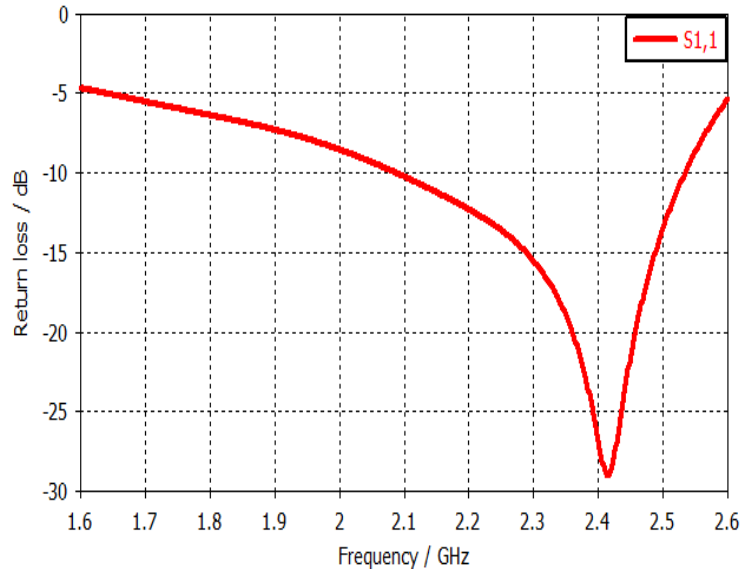


Figure 4: Return loss plot of the optimized slotted patch antenna

3. MIMO ANTENNA DESIGN

3.1 Basic Design

MIMO antenna can be created by doubling the substrate, the ground plane, and the radiated patch. A compact MIMO is therefore obtained, as shown in Figure 5, with dimensions ($L_g \times W_g \times h$) of $(48 \times 48 \times 1.6) \text{mm}^3$. The partial ground length L_{g1} of 15.4mm is obtained through optimization process to maintain the resonance frequency at 2.4GHz.

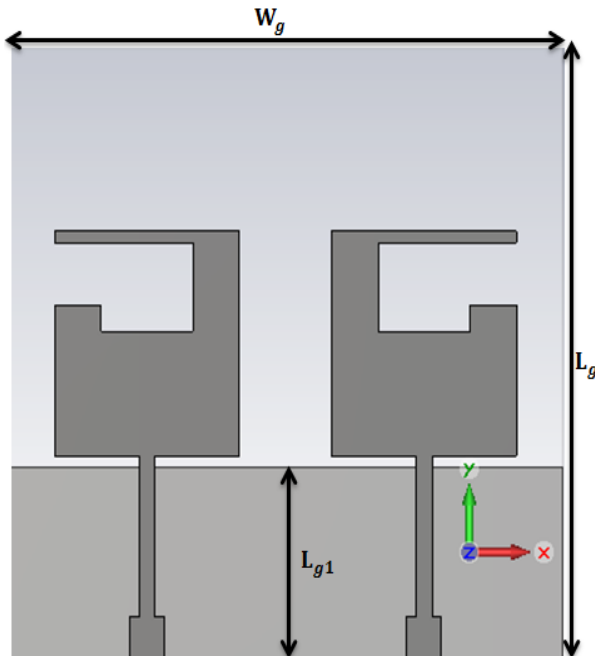


Figure 5: Compact MIMO antenna

The s-parameter simulation result is shown in Figure 6. The return loss (S_{11}) has a good value of -35.7dB at 2.4GHz and a bandwidth of 485MHz. However, the mutual coupling (S_{21}) has a high value of -6.66dB at 2.4GHz, which needs to be decreased by using parasitic element technique. The total gain of the MIMO antenna is shown in Figure 7, with a relatively good value of 2dBi at 2.4 GHz.

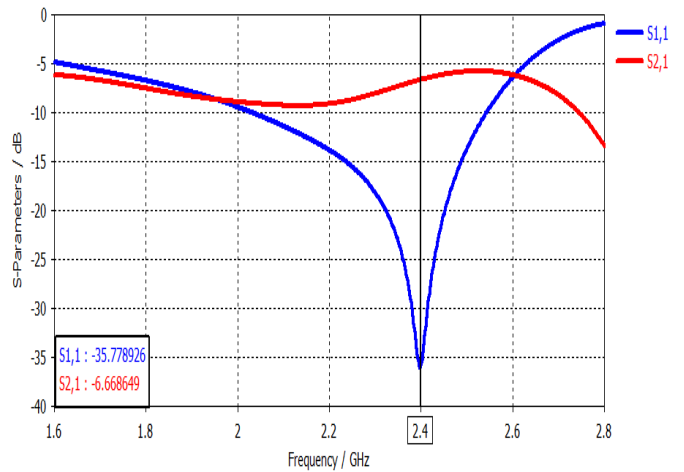


Figure 6: S-parameter simulation result of MIMO antenna

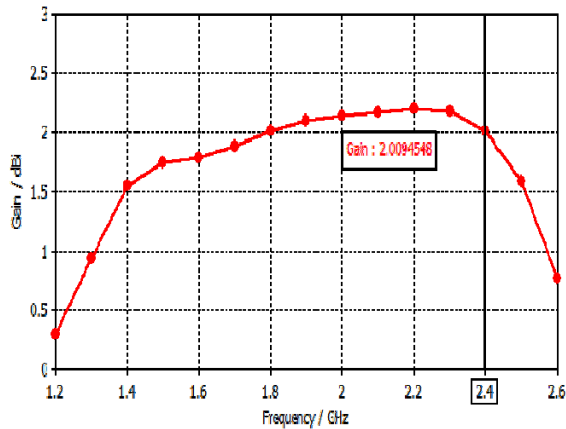


Figure 7: Total gain plot vs. frequency of MIMO antenna.

3.2 Parasitic Element Technique

Parasitic element is an element with certain shape and size inserted between MIMO elements (non-physical connected)[13-15] or connected to the ground plane as a resonator[16-20]. In this paper, a non-physical connected parasitic element is used to reduce the mutual coupling between the MIMO elements. This parasitic element will create an opposite coupling field on its both sides so as to reduce the original field, therefore reducing the overall coupling. As shown in Figure 8, $I_{excited1}$ is referred to as the exciting current feeding to element 1, $I_{coupling_par}$ denotes the coupling current between the patches and parasitic element, and $I_{coupling2}$ is the coupling current between patch elements 1 and 2. The overall coupling current $I_{coupling}$ on the victim antenna can be expressed by [13].

$$I_{coupling} = (-\alpha + \beta^2)I_{excited} \quad (5)$$

Where (α) represents the coupling factor between patch elements 1 and 2, and (β) represents the coupling factor between parasitic element and element 1. It is clear from Equation 5 that if $(- \alpha + \beta^2)$ has right tuning value and becomes approximately equal to 0, then the $I_{coupling}$ could be eliminated.

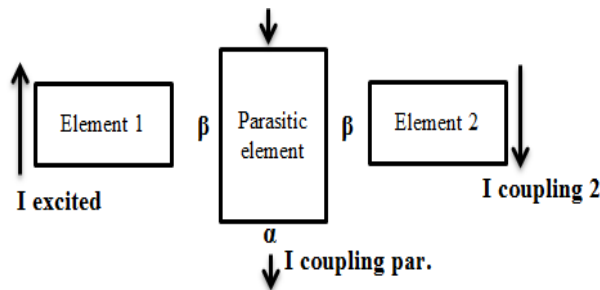


Figure 8:Block diagram of parasitic element operation

3.3 Parasitic Element Design

In this paper, a novel design of parasitic element is proposed, which has a rectangular shape with square slots as shown in Figure 9.

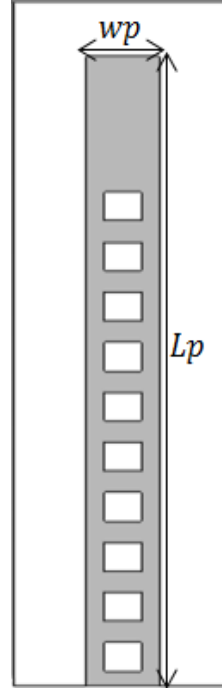


Figure 9:Geometric shape of the proposed parasitic element

Firstly, parasitic element of and without slots is tested by using frequency domain method. The parasitic element is inserted between two-port waveguide as shown in Figure 10. The spacing between the planar waveguide and the closely side of the parasitic element is adjusted and optimized by the CST software.

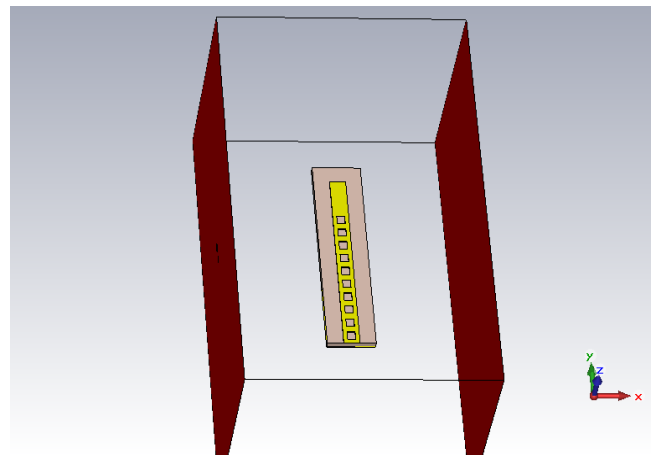


Figure 10:Frequency simulation setup of parasitic element

<http://www.cisjournal.org>

The parasitic element is printed on FR4 substrate with $L = 48$ mm and $W = 6$ mm. A partial ground plane is used with $W_g = 15.4$ mm, which is equal to the space between MIMO elements in the original structure in order to make parasitic element more compactable. The s-parameter characteristic of this parasitic element is shown in Figure 11 with a minimum $S_{21} = -7$ dB at 5.35 GHz. The latter value is relatively high and needs to be reduced. The resonance frequency also needs to be shifted to 2.4 GHz.

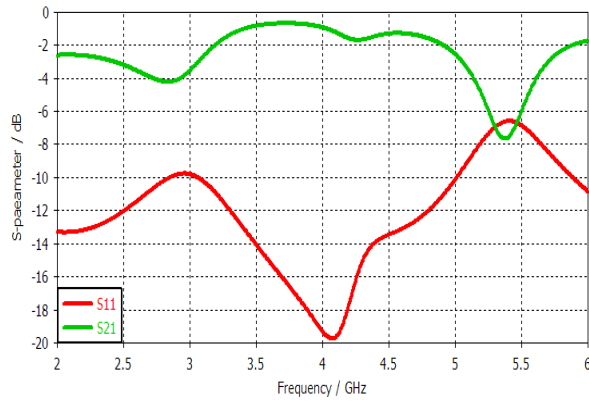


Figure 11: S-parameter simulation results of parasitic element

The improvement process can be done by creating several square slots in the parasitic element. A parametric study has to be conducted on the parasitic element, and the key parameters in this study are length

(and width (of the parasitic element, slot length(x_1), number of slots (N). Linear process is achieved by changing every parameter while keeping the others constant. The s-parameter simulation results are shown in Figure 12 and Table 3.

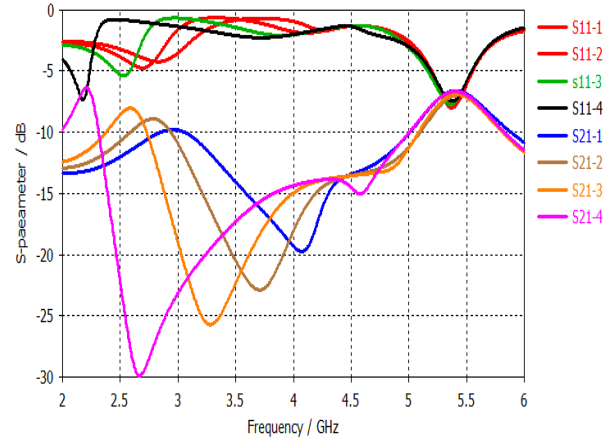


Figure 12: S-parameter simulation results for different parameter values

Table 3: Various parameter values extracted from the parametric study.

S ₁₁ curve	S ₂₁ curve	L _p (mm)	W _p (mm)	N	X ₁	Min. S ₁₁ (dB)	Min. S ₂₁ (dB)
S ₁₁ -1	S ₂₁ -1	20	6	0	0	-1.1	-19.7
S ₁₁ -2	S ₂₁ -2	30	5.5	3	0.5	-1.1	-22.8
S ₁₁ -3	S ₂₁ -3	36	4.5	5	0.8	-0.9	-25.7
S ₁₁ -4	S ₂₁ -4	44	4	10	1	-0.96	-29.8

The optimum s-parameter characteristics shown in Figure 13, are found with, $x_1 = 1$ mm, $N = 10$. The

prototype MIMO antenna is fabricated according to the above dimensions as shown in Figure 14.

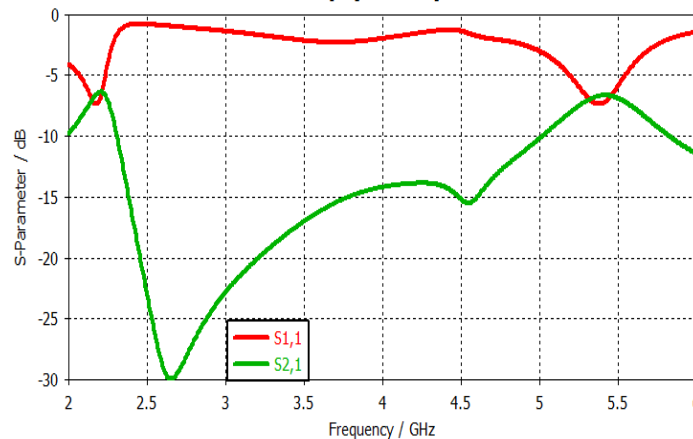
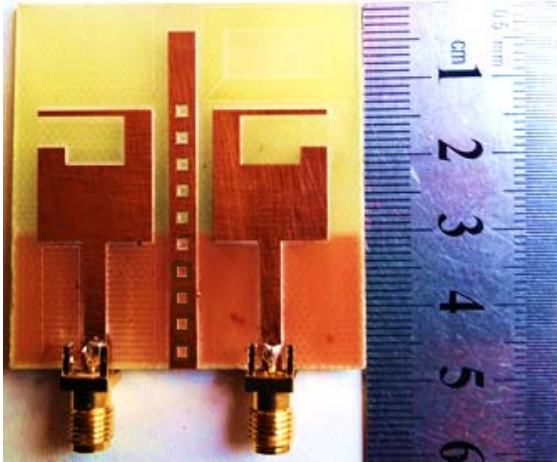
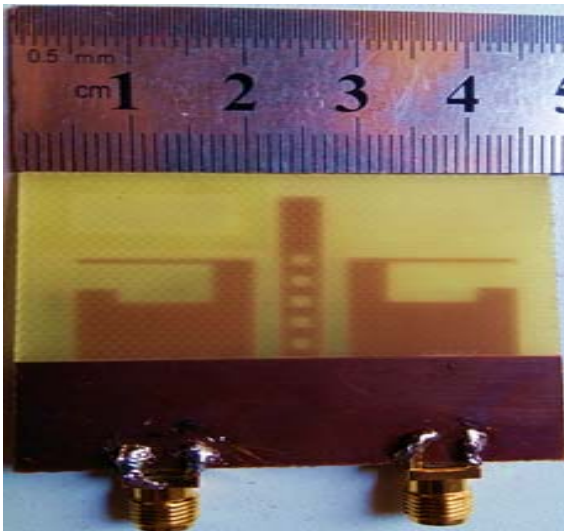


Figure 13: The optimum s-parameter characteristics

<http://www.cisjournal.org>



(a)



(b)

Figure 14: The fabricated MIMO antenna (a) Front view, (b) Back view.

3.3 Results

A. Surface Current

The surface current distribution with and without parasitic element is shown in Figure 15. It is clear that higher surface current is flowing between MIMO elements, while adding the parasitic element help in reducing it.

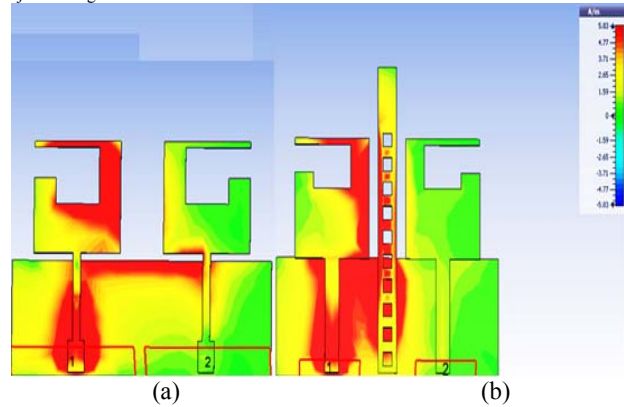


Figure 15: Surface current (a) without parasitic element (b) with parasitic element

B. S_{11} -Parameter

Figure 16 shows the simulated and measured S_{11} parameter with and without parasitic element. It can be observed that the impedance matching is improved with parasitic element. However, the bandwidth is decreased to 450MHz (i.e. percentage of 18.75%). This decrease is attributed to the effect of adding parasitic element.

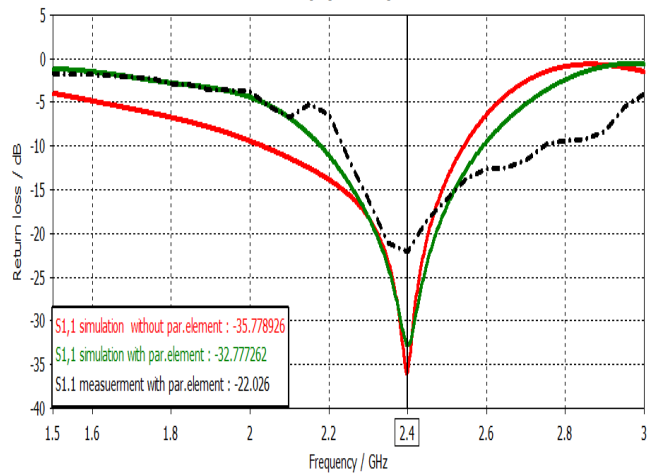


Figure 16: Simulated and measured S_{11} parameter

C. S_{21} -Parameter

As shown in Figure 17, the simulated mutual coupling has been decreased from -6.668dB to -33dB with the adding of parasitic element in the band of interest.

There is small difference between simulation and measurement results due to the fabrication error.

http://www.cisjournal.org

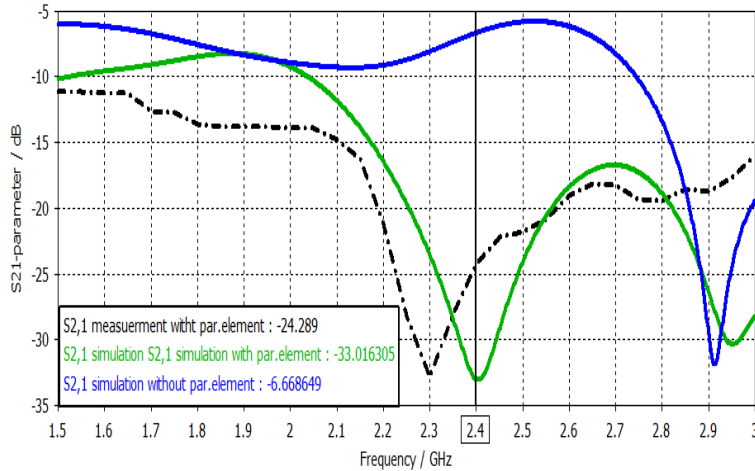


Figure 17: Simulated and measured of S₂₁-parameter

D. Envelope Correlation Coefficient (ρ_e)

It is an important parameter that gives a measure to how much the MIMO channels are isolated or correlated with each other. The best performance in MIMO systems, (ρ_e) must be less than 0.5 and can be calculated using s-parameter as[21] :

$$\rho_e = \frac{|S_{11} + S_{12} + S_{22}S_{21}^{-1}|^2}{(1 - (|S_{11}|^2 + |S_{21}|^2))(1 - (|S_{22}|^2 + |S_{12}|^2))} \quad (6)$$

The simulated and measured envelope correlation coefficients are shown in Figure 18. It is clear that ρ_e is less than 0.1 in the band of interest (2.1-2.6) GHz.

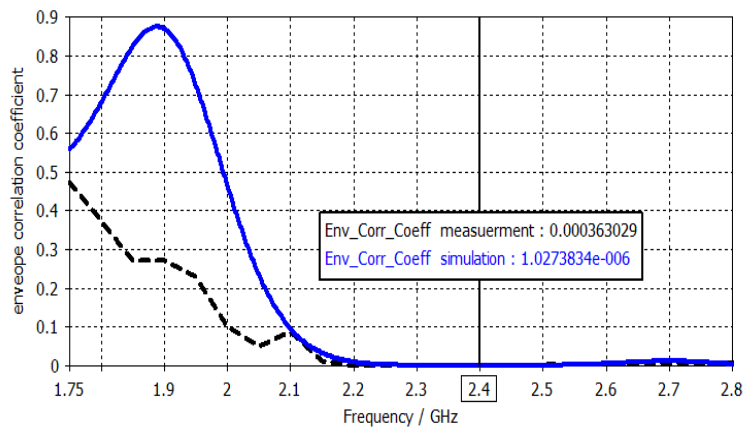


Figure 18: Simulated and measured results of envelope correlation coefficient

E. Gain

The simulated and measured gain values with and without the parasitic element are shown in Figure 19.

Using of parasitic element has increased the gain from 2dBi to 2.35dBi, and generally there is a reasonable agreement between simulated and measured results.

http://www.cisjournal.org

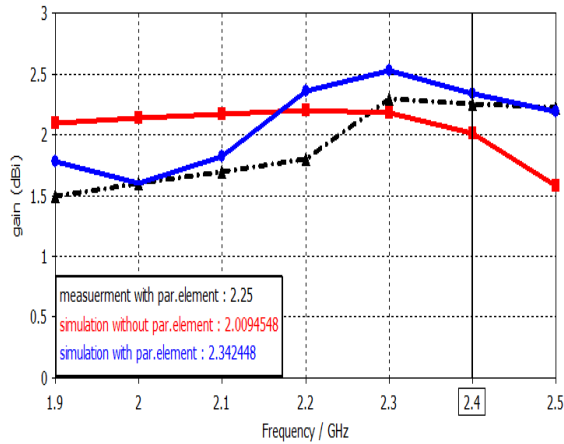


Figure 19: Simulated and measured gain values

F. Total Efficiency η_{tot}

It is another important parameter that affects the mutual coupling and can calculate as [9]

$$\eta_{tot} = \eta_{radiation} \times \eta_{(mismatch+coupling)} \quad (7)$$

where

$$\eta_{(mismatch+coupling)} = 1 - |s_{11}|^2 - [s_{21}^2 + s_{12}^2] \quad (8)$$

The simulated and measured values of η_{tot} with and without the parasitic element are shown in Figure 20. A noticeable increase of η_{tot} has been achieved with using of parasitic element. The measured value of η_{tot} is found as 89.5%.

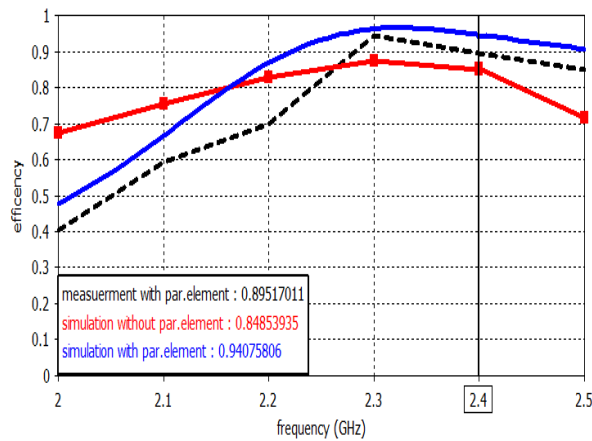
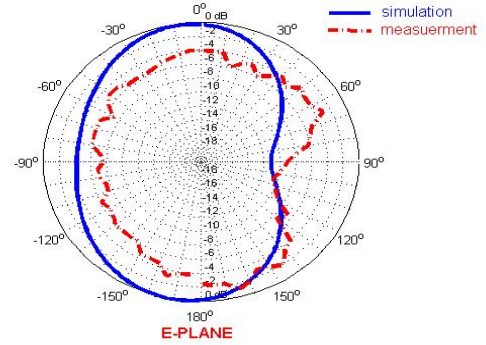


Figure 20: Simulation and measured efficiency values with/without parasitic element

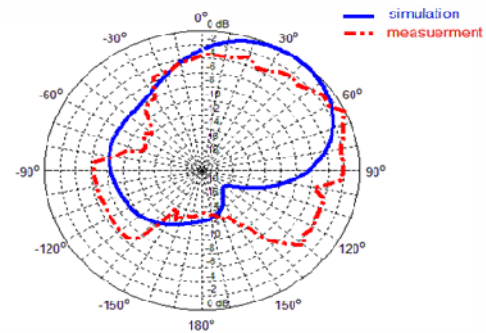
G. Radiation Patterns

The simulated and measured radiation patterns at 2.4 GHz are shown in Figure 21. The E-plane pattern is

shifted to the left due to the presence of the parasitic element. The H-plane pattern has a lower back lobe compared with E-plane. It should be mentioned that the E-plane pattern of Figure 21 is due to one element and the pattern of the other element is shifted to the right.



(a)



(b)

Figure 21: Simulation and measurement radiation patterns: (a) E-plane (b) H-plane

4. CONCLUSION

In this paper, the simulation, fabrication and testing of a (2x1) MIMO antenna system of compact size of (48x48x1.6) mm³ is presented. This antenna is fabricated on FR-4 dielectric substrate with $\epsilon_r=4.4$ and loss tangent $\tan\delta=0.025$ to work at 2.4GHz for WLAN applications. A novel rectangular parasitic element structure with (10) square slots is proposed to reduce the mutual coupling to about -25dB at 2.4GHz. Other parameters such as total efficiency, gain and bandwidth are all enhanced with the adding of the proposed parasitic element.

REFERENCES

[1] M. S. Sharawi, Printed MIMO antenna engineering. Artech House, Inc., 2014.
[2] E. Biglieri, R. Calderbank, A. Constantinides, A. Goldsmith, A. Paulraj, H. V. Poor, MIMO wireless communications. Cambridge University Press, 2007.

<http://www.cisjournal.org>

- [3] K. J. Babu, K. Krishna, L. P. Reddy, "A review on the design of MIMO antennas for upcoming 4G communications", *International Journal of Applied Engineering Research*, Dindigul, Vol.1, No.4, pp.85-93, 2011.
- [4] A. A. Abouda, S. Häggman, "Effect of mutual coupling on capacity of MIMO wireless channels in high SNR scenario", *Progress In Electromagnetics Research*, Vol.65, pp.27-40, 2006.
- [5] H. Nigam, M. Kumar, "A Compact MIMO Antenna Design for 2.4 GHz ISM Band Frequency Applications", *International Journal of Electronics and Computer Science Engineering*, pp.324-331, 2014.
- [6] W. Marzudi, Z. Abidin, S. Muji, M. Yue, R. A. Abd-Alhameed, "Minimization of mutual coupling using neutralization line technique for 2.4 GHz wireless applications", *International Journal of Digital Information and Wireless Communications (IJDWC)*, Vol.4, pp.292-298, 2014.
- [7] Y. Lee, D. Ga, J. Choi, "Design of a MIMO antenna with improved isolation using MNG metamaterial", *International Journal of Antennas and Propagation*, Vol.2012, pp.1-7, 2012.
- [8] M. Alsath, M. Kanagasabai, B. Balasubramanian, "Implementation of slotted meander-line resonators for isolation enhancement in microstrip patch antenna arrays", *IEEE Antennas and Wireless Propagation Letters*, Vol.12, pp.15-18, 2013.
- [9] C. A. Balanis, *Antenna theory: analysis and design. MICROSTRIP ANTENNAS*, 3rd edition, John Wiley & sons, 2005.
- [10] M.S. Karoui, H. Ghariani, M. Samet, M. Ramdani, R. Perdriau, "Bandwidth Enhancement of the Square patch antenna for bio telemetry Applications", *International Journal of Information Systems and Telecommunication Engineering*, Vol.1, pp.12-18, 2010.
- [11] L. Huitema, T. Monediere, *Progress in Compact Antennas*, In Tech publishing House, 2014.
- [12] CST: *Computer Simulation Technology Based on FIT Method*, CST Computer Simulation Technology, 2011.
- [13] A. C. Mak, C. R. Rowell, R. D. Murch, "Isolation enhancement between two closely packed antennas", *IEEE Transactions on Antennas and Propagation*, Vol.56, pp.3411-3419, 2008.
- [14] Z. Li et al., "Reducing Mutual Coupling of MIMO Antennas with Parasitic Elements for Mobile Terminals," *IEEE Antennas and Wireless Propagation Letters*, Vol.60, No.2, pp.473-481, 2012.
- [15] K. S. Min, D. J. Kim, and Y. M. Moon, "Improved MIMO Antenna by Mutual Coupling Suppression Between Elements," *Proc. European Conf. on Wireless Technology*, pp.125-128, 2005.
- [16] M. G. N. Alsath, M. Kanagasabai, and B. Balasubramanian, "Implementation of Slotted Meander-Line Resonators for Isolation Enhancement in Microstrip Patch Antenna Arrays," *IEEE Antennas and Wireless Propagation Letters*, Vol.12, pp.15-18, 2013.
- [17] S. Yoo and S. Kahng, "A Compact MIMO Antenna Using ZOR Split Ring Resonator Radiators with a Decoupling Structure," *Microwave Journal*, Vol.54, No.11, pp.1-11, 2011.
- [18] M. S. Khan et al., "Compact UWB-MIMO Antenna Array with a Novel Decoupling Structure," *Proc. 10th Int. Bhurban Conference on Applied Sciences & Technology*, pp.347-350, 2013.
- [19] C. H. Lee, S. Y. Chen, and P. Hsu, "Integrated Dual Planar Inverted-F Antenna with Enhanced Isolation," *IEEE Antennas and Wireless Propagation Letters*, Vol.8, pp.963-965, 2009.
- [20] T. W. Kang and K. L. Wong, "Isolation Improvement of WLAN Internal Laptop Computer Antennas Using Dual-Band Strip Resonator," *Proc. Asia-Pacific Microwave Conference*, pp. 2478-2481, 2009.
- [21] S. Blanch, J. Romeu, I. Corbella, "Exact representation of antenna system diversity performance from input parameter description," *Electronics letters*, Vol.39, pp.705-707, 2003.